JOURNAL OF
Materials
CHEMISTRY

Control of mesostructured silica particle morphology

Henry B. S. Chan,[a] **Peter M. Budd***[a] **and Timothy deV. Naylor**[b]

[a] *Department of Chemistry, University of Manchester, Manchester, UK M13 9PL.*
E-mail: Peter.Budd@man.ac.uk
[b] *Smart Chemical Company Ltd., Unit 5, Blatchford Road, Horsham, W. Sussex, UK RH13 5QR*

Received 14th July 2000, Accepted 19th December 2000
First published as an Advance Article on the web 30th January 2001

The formation of mesostructured silica was investigated using acidic conditions with tetraethoxysilane (TEOS) as the silica precursor and cetyltrimethylammonium bromide (CTAB) as the structure directing agent. A synthesis mixture of composition 2.2TEOS : 1.1CTAB : 75HCl : $1000H_2O$ gave a well ordered material exhibiting a range of particle shapes from extended rope-like structures of hexagonal cross-section to gyroid structures. Addition of monomethyltriethoxysilane (MTES) or tetrahydrofuran (THF) to the synthesis mixture gave rise to spherical particles. Studies of particle development showed initial growth of gel-like particles within which the mesostructure developed. A new model is proposed for the formation of mesostructured precipitates in which (1) growth of inorganic oligomers gives rise to a thermodynamically unstable mixture, (2) phase separation occurs giving droplets of a second liquid (or liquid crystal) phase rich in oligomer and surfactant, (3) the droplets are colloidally stabilized, (4) microphase separation occurs within the droplets, giving rise to a mesostructure and (5) further polymerization fixes the mesostructure.

Introduction

Zeolites and other microporous materials, which have regular arrays of pores and channels with dimensions <2 nm, find extensive use in catalysis and as ion exchangers and selective adsorbents. The challenge in recent years has been to extend the range of ordered nanoporous materials into the mesopore size range (2–10 nm) for application in separations and reactions involving large molecules, as chromatography media, for controlled release of agrochemicals and as hosts for supramolecular assembly. A major advance was the development at Mobil corporation of the M41S family of mesostructured silicas.[1–3] Cationic surfactants were used as structure directing agents and hexagonal (MCM-41), cubic (MCM-48) and lamellar (MCM-50) materials were obtained. Removal of the surfactant by calcination gave mesoporous products. Over the past few years, a wide variety of surfactant types have been similarly used to generate a range of mesoporous metal oxide structures. For example, we have utilised poly(oxyethylene)/poly(oxybutylene)/poly(oxyethylene) triblock copolymers in the preparation of mesoporous silica.[4]

For practical application, the overall morphology of a mesoporous material may be as important as its internal structure. For example, if the material is to be used as column packing, spherical particles are preferred to irregular particles, which tend to break down. Huo *et al.*[5] prepared large (*ca.* 0.5 mm diameter) mesoporous silica spheres using tetrabutoxysilane as a silica precursor. Yang *et al.*[6] have reported the synthesis of mesoporous silica spheres under conditions of low acidity.

In the present work, factors that influence the morphology of mesostructured silica particles were explored. Mesostructured silica was prepared under acid conditions with tetraethoxysilane (TEOS) as the silica precursor and cetyltrimethylammonium bromide (CTAB) as the structure directing agent. Synthesis conditions were found which gave particles for which a high degree of internal hexagonal order (MCM-41 type) was reflected in the external morphology. Two novel routes to microspheres were investigated: (1) incorporation of a small proportion of a second silica precursor, monomethyltriethoxysilane (MTES) into the synthesis mixture and (2) addition of a water-miscible cosolvent, tetrahydrofuran (THF). The results are discussed in the context of a new model of the formation of mesostructured precipitates.

Experimental

Preparation of mesostructured silica

A representative synthesis is given below, for which the mole ratio of the initial mixture is 2.2TEOS : 1.1CTAB : 75HCl : $1000H_2O$. Other syntheses were carried out with different proportions of the reagents, and with the inclusion of MTES or THF, as summarised in Tables 1–3.

CTAB (Aldrich) (2.68 g) was dissolved with stirring in a mixture of distilled water (88.3 g) and concentrated hydrochloric acid (49.2 g, 37 wt% HCl). TEOS (Aldrich) (3.06 g) was added rapidly with vigorous stirring and stirring stopped after a further 45 s, when a clear solution had formed. For syntheses including MTES (Lancaster) or THF, this was first mixed with the TEOS. The mixture was aged at room temperature under static conditions for 18 h. Precipitated solids were filtered off, washed with distilled water (5×100 cm^3) and allowed to dry. Calcination was carried out in a tube furnace, heating in flowing nitrogen at 1 °C min^{-1} to 540 °C, maintaining that temperature for 6 h, then repeating the procedure in flowing air.

Characterization

Scanning electron microscopy (SEM) was undertaken with a JEOL 640 instrument. Samples were gold-coated for SEM using an International Scientific Instruments PS-2 coating unit. X-Ray diffraction (XRD) was carried out using a Philips PW 1730 generator (CuKα, $\lambda=1.54$ pm) and Philips PW 1050 goniometer. Polarized optical microscopy was carried out with a Nikon Optishot microscope. Magic angle spinning ^{29}Si NMR was carried out with a Varian Unity 300 instrument. Nitrogen

DOI: 10.1039/b005713o

Table 1 Effect of varying surfactant and acid concentrations on morphology and X-ray diffraction pattern

Sample	Mole ratio TEOS : CTAB : HCl : H_2O	Appearance in SEM	XRD d-spacing/Å				
FA85	2.2 : 0.28 : 75 : 1000	C		39.4	22.9		
FA81	2.2 : 0.55 : 75 : 1000	C/R		38.9			
FA60	2.2 : 1.1 : 75 : 1000	C_h/R_h/G		36.3	21.1	18.3	13.0
			cal:	33.7	19.4	16.8	
FA82	2.2 : 2.2 : 75 : 1000	C/R		37.6			
FA83	2.2 : 4.4 : 75 : 1000	C/R		37.8			
FA46	1.1 : 0.55 : 37.5 : 1000	I		36.9	21.2		
FA48	1.1 : 0.55 : 9.5 : 1000	I/G		40.2	26.1	24.1	13.0
FA49	1.1 : 0.55 : 4.7 : 1000	I/G		39.9	26.1	23.2	13.0

XRD is for as-synthesised materials except where indicated cal (calcined). KEY: C = curled structures, R = extended rope-like structures, C_h = curled structures with hexagonal cross-section, R_h = extended rope-like structures with hexagonal cross-section, G = gyroid structures, I = irregular particles.

adsorption/desorption analysis was undertaken using a Gemini 2375 instrument at the University of Greenwich.

Results

Particles with hexagonal morphology

A synthesis mixture of composition 2.2TEOS : 1.1CTAB : 75HCl : $1000H_2O$ was found to give a product with a high degree of internal hexagonal order, as indicated by the XRD pattern (Table 1, d-spacings in the ratio $1:(1/\sqrt{3}):(1/\sqrt{4}):(1/\sqrt{7})$), which was reflected in the external morphology of the particles, as observed by SEM (Fig. 1). A variety of particle shapes was obtained, ranging from extended rope-like and curled structures of hexagonal cross-section, to gyroid structures with well-defined facets. Similar morphologies have been reported by Yang *et al.*[7] On calcination there was some shrinkage, but both the internal order and external morphology were retained. The material exhibited birefringence when observed by polarised optical microscopy, confirming the pore structure to be anisotropic.

The nitrogen adsorption/desorption isotherm (Fig. 2) of the calcined material was typical of mesoporous silica prepared under acidic conditions.[6] It has been noted previously that acid prepared mesostructures exhibit different sorption behaviour to M41S samples of similar lattice spacing prepared under alkaline conditions, with a step in the isotherm at much lower p/p^o values, indicating either rippled surfaces or the presence of micropores.[8] BET analysis gave a surface area of 1220 $m^2\,g^{-1}$, demonstrating a high degree of porosity.

The effects of varying the proportions of surfactant and acid in the synthesis mixture are indicated in Table 1. Changing the surfactant concentration gave less well ordered materials, as indicated by a reduced number of peaks in the XRD pattern. On reducing the acidity a change in the XRD pattern was observed, but it was not possible conclusively to assign a structure.

Effect of incorporation of MTES

A synthesis mixture of composition 2.0TEOS : 0.25MTES : 1.1CTAB : 75HCl : $1000H_2O$ gave particles of spherical morphology, which was retained on calcination (Fig. 3). The XRD pattern of as-synthesised microspheres (Fig. 4a) exhibited two major peaks as well as minor peaks. This may be interpreted either as a single distorted hexagonal (orthorhombic) structure or as a mixture of two hexagonal structures. Further evidence is required to distinguish conclusively between these two possibilities. Calcination led to a reduction in the d-spacings of the major peaks and the loss of the minor peaks (Fig. 4b and Table 2), suggesting some shrinkage and a reduction in the degree of internal order.

^{29}Si solid state NMR of as-synthesised products showed peaks in the region of -60 ppm, which can be attributed to units containing a Si–CH_3 bond (T_2, T_3 units), as well as peaks around -100 ppm, which can be attributed to units containing only Si–O– bonds (Q_2, Q_3, Q_4 units).[9] On increasing the proportion of MTES in the synthesis mixture, the relative intensity of the signals around -60 ppm increased. On calcination, these signals were lost. This indicates that methyl groups were incorporated into the framework during synthesis and were lost on calcination.

Particle size distributions for as-synthesised and calcined microspheres are shown in Fig. 5. The particles did not exhibit optical birefringence. The nitrogen adsorption/desorption

Table 2 Effect of addition of MTES on morphology and X-ray diffraction pattern

Sample	Mole ratio TEOS : MTES : CTAB : HCl : H_2O	Appearance in SEM	XRD d-spacing/Å					
MSA42	2.1 : 0.09 : 1.1 : 75 : 1000	C/R/G		34.3		20.5		13.0
MSA43	2.1 : 0.16 : 1.1 : 75 : 1000	C/S		34.8		20.2	17.5	13.1
MSA40	2.0 : 0.25 : 1.1 : 75 : 1000	S		37.6	35.2	22.9	17.3	13.1
			cal:	34.1	31.4			
MSA45	1.9 : 0.31 : 1.1 : 75 : 1000	S		37.1	34.0	22		
MSA65	1.9 : 0.26 : 2.15 : 73 : 1000	C/R		35.5	32.7			
MSA66	1.9 : 0.26 : 0.54 : 73 : 1000	S		38.5	35.2	24		
MSA67	1.9 : 0.26 : 0.22 : 73 : 1000	S		37.0	34.0	23		
MSA71	5.9 : 0.73 : 1.1 : 75 : 1000	S		38.3				
MSA72	4.0 : 0.49 : 1.1 : 75 : 1000	S		38.1	34.8	23		
MSA73	1.0 : 0.13 : 1.1 : 75 : 1000	S/I		39.0	35.9	24		
MSA74	0.65 : 0.10 : 1.1 : 75 : 1000	S/I		39.5	36.3	25		
MSA75	0.50 : 0.07 : 1.1 : 75 : 1000	S/I		39.3	36.2	25		
MSA77	2.1 : 0.31 : 1.2 : 66 : 1000	C/S		34.8		20		
MSA78	2.0 : 0.29 : 1.1 : 45 : 1000	I		35.3	26	20		13
MSA79	2.0 : 0.29 : 1.1 : 37 : 1000	I/G		34.7		20	17	13

XRD is for as-synthesised materials except where indicated cal (calcined). KEY: I = irregular particles, S = spherical particles, R = extended rope-like structures, G = gyroid structures, C = curled structures.

Table 3 Effect of addition of THF on morphology and X-ray diffraction pattern

Sample	Mole ratio TEOS : CTAB : THF : HCl : H_2O	Appearance in SEM	XRD *d*-spacing/Å					
MSB35	2.2 : 1.1 : 4 : 75 : 1000	I		36.2	20.9	18	14	13
MSB37	2.2 : 1.1 : 13 : 75 : 1000	I		34.8	20.0	17		13
MSB36	2.2 : 1.1 : 17 : 75 : 1000	I		34.0	19.4	17		
MSB34	2.2 : 1.1 : 21 : 75 : 1000	S		36.1	21.2			
			cal:	34.4	20.9			
MSB38	2.2 : 1.1 : 31 : 75 : 1000	S		35.3		17		
MSB59	2.2 : 0.28 : 21 : 75 : 1000	S (aggregated)		36.3				
MSB60	2.2 : 0.56 : 21 : 75 : 1000	S (aggregated)		37.0				
MSB61	2.2 : 2.22 : 21 : 75 : 1000	S/I		34.7				
MSB62	2.2 : 4.44 : 21 : 75 : 1000	I		34.7				
MSB64	8.9 : 1.1 : 30 : 75 : 1000	S		36.6				
MSB66	4.4 : 1.1 : 42 : 75 : 1000	S		35.0				
MSB67	1.1 : 1.1 : 11 : 75 : 1000	R/G		34.6				

XRD is for as-synthesised materials except where indicated cal (calcined). KEY: I = irregular particles, S = spherical particles, R = extended rope-like structures, G = gyroid structures.

isotherm of calcined microspheres was very similar to that for particles with hexagonal morphology and the BET surface area was 910 $m^2\ g^{-1}$.

The effects of varying the proportions of MTES, CTAB and HCl in the synthesis mixture are indicated in Table 2. Some experiments were also carried out in which the mixture was stirred for extended periods during synthesis, but this gave rise to highly aggregated products.

Effect of addition of THF

A synthesis mixture of composition 2.2TEOS : 1.1CTAB : 21THF : 75HCl : $1000H_2O$ gave particles of spherical morphology, which was retained on calcination (Fig. 6). The XRD patterns of as-synthesised and calcined microspheres (Fig. 7) exhibited two peaks which could be ascribed to a hexagonal structure and, in contrast to spheres formed on incorporation of MTES, there was only a slight reduction in *d*-spacing on calcination. Particle size distributions for as-synthesised and calcined microspheres are shown in Fig. 8. The nitrogen adsorption/desorption isotherm of calcined microspheres was very similar to that for particles with hexagonal morphology and the BET surface area was 800 $m^2\ g^{-1}$.

The effects of varying the proportions of THF and CTAB in the synthesis mixture are indicated in Table 3. The effect of increasing THF content on the XRD pattern of the product is illustrated in Fig. 9.

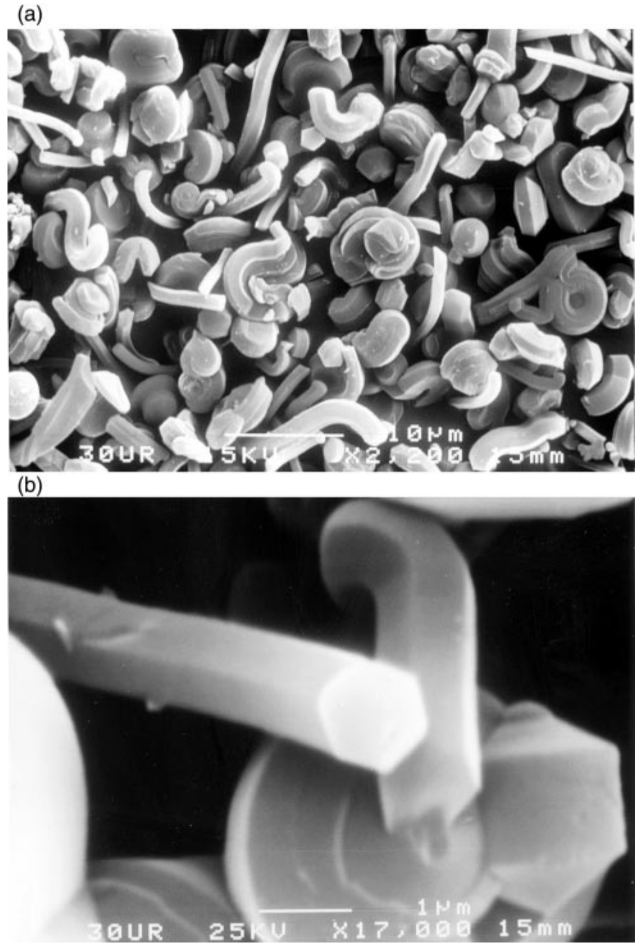

Fig. 1 Scanning electron micrographs of calcined silica from a synthesis mixture of composition 2.2TEOS : 1.1CTAB : 75HCl : $1000H_2O$ at (a) low magnification and (b) high magnification.

Particle development

Particle development was studied (1) by direct observation of a small amount of the synthesis mixture under an optical microscope and (2) by SEM and XRD of samples isolated at intervals from the synthesis mixture.

For a synthesis mixture of composition 2.2TEOS : 1.1 CTAB : 75HCl : $1000H_2O$, which ultimately gave rise to a mixture of particles with hexagonal morphology (Fig. 1), particles could be detected by optical microscopy 3 min after the start of the ageing period. The particles rapidly grew and had reached approximately their final size within 7 min. Electron micrographs of samples isolated at times from 15 min (Fig. 10a) to 24 h (Fig. 10b) showed the particles to develop more pronounced facets over that period, but not to

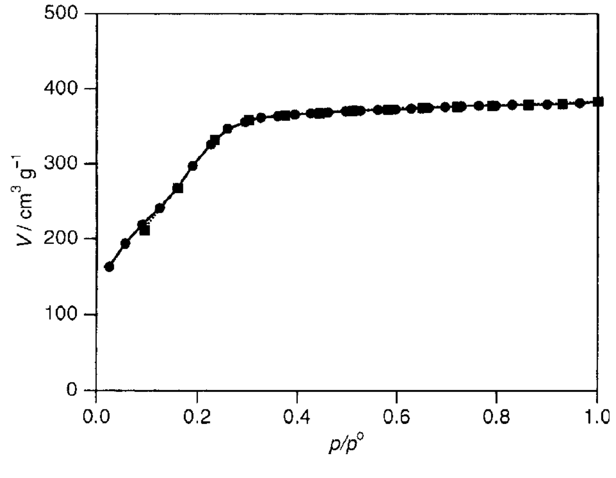

Fig. 2 Nitrogen adsorption (circles) and desorption (squares) isotherm of calcined silica from a synthesis mixture of composition 2.2TEOS : 1.1CTAB : 75HCl : $1000H_2O$.

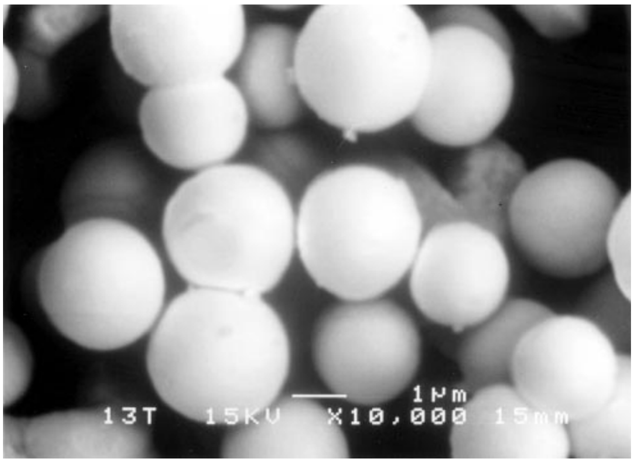

Fig. 3 Scanning electron micrograph of calcined silica microspheres from a synthesis mixture of composition 2.0TEOS : 0.25MTES : 1.1CTAB : 75HCl : $1000H_2O$.

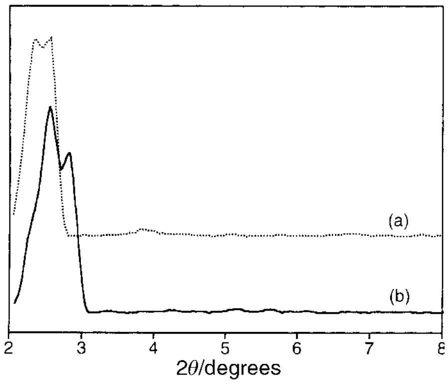

Fig. 4 X-Ray diffraction patterns of (a) as-synthesised and (b) calcined silica microspheres from a synthesis mixture of composition 2.0TEOS : 0.25MTES : 1.1CTAB : 75HCl : $1000H_2O$.

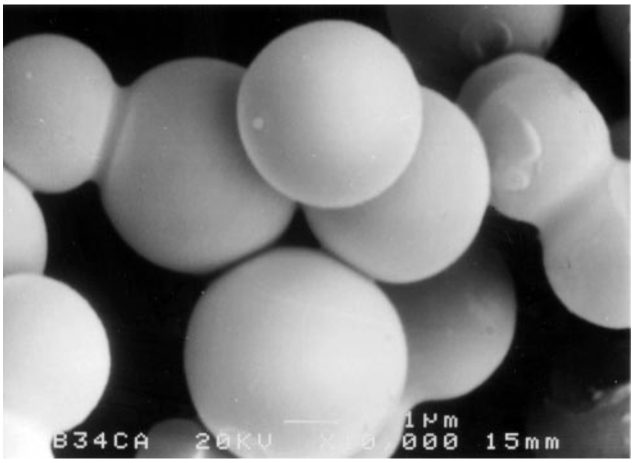

Fig. 6 Scanning electron micrograph of calcined silica microspheres from a synthesis mixture of composition 2.2TEOS : 1.1CTAB : 21THF : 75HCl : $1000H_2O$.

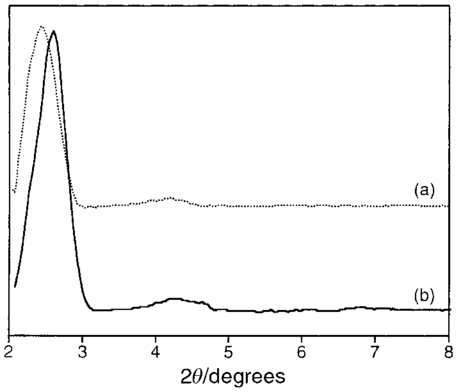

Fig. 7 X-Ray diffraction patterns of (a) as-synthesised and (b) calcined silica microspheres from a synthesis mixture of composition 2.2TEOS : 1.1CTAB : 21THF : 75HCl : $1000H_2O$.

change significantly in size. No XRD peaks were observed for material isolated after 15 min, but the XRD pattern developed subsequently, as can be seen in Fig. 11.

For a synthesis mixture including MTES (composition 2.0TEOS : 0.25MTES : 1.1CTAB : 75HCl : $1000H_2O$), which ultimately gave rise to microspheres (Fig. 3), particles could be detected by optical microscopy 8 min after the start of the ageing period, and had reached approximately their final size after 16 min. SEM also showed a rapid increase in particle size during the first few minutes of the ageing process, as can be seen in Fig. 12. After 1 h, the XRD pattern showed three peaks (*d*-spacings: 38.3 Å, 35.3 Å, 23 Å). Attempts to filter particles before 1 h gave rise to a gel-like layer which appeared amorphous by XRD.

For a synthesis mixture including THF (composition 2.2TEOS : 1.1CTAB : 21THF : 75HCl : $1000H_2O$), which also gave particles of spherical morphology (Fig. 6), growth was slower. Under the optical microscope, particles could be observed after 23 min, which then grew. SEM indicated the particles to have reached nearly their final size after 3 h, as can be seen in Fig. 13. After 30 min a single, broad XRD peak was obtained. Attempts to filter particles before 30 min gave rise to a gel-like layer which appeared amorphous by XRD.

The picture that emerges is that of initial growth of gel-like,

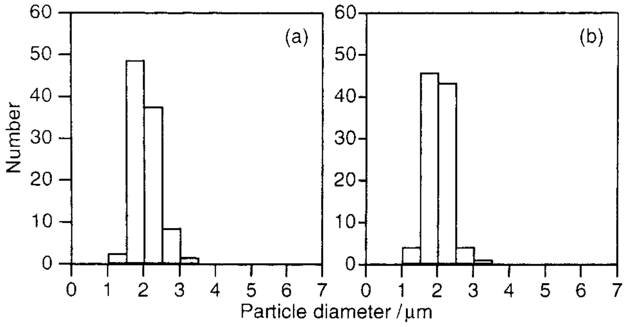

Fig. 5 Particle size distributions of (a) as-synthesised and (b) calcined silica microspheres from a synthesis mixture of composition 2.0TEOS : 0.25MTES : 1.1CTAB : 75HCl : $1000H_2O$.

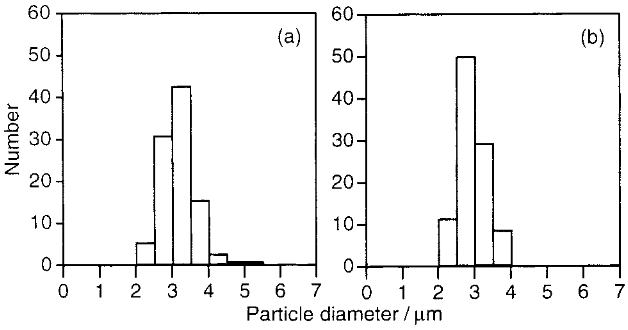

Fig. 8 Particle size distributions of (a) as-synthesised and (b) calcined silica microspheres from a synthesis mixture of composition 2.2TEOS : 1.1CTAB : 21THF : 75HCl : $1000H_2O$.

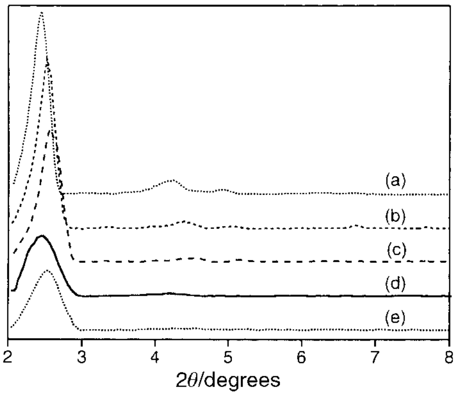

Fig. 9 X-Ray diffraction patterns of as-synthesised products from synthesis mixtures of composition 2.2TEOS : 1.1CTAB : xTHF : 75HCl : 1000H_2O, where x is (a) 4, (b) 13, (c) 17, (d) 21 and (e) 31.

colloidally-stabilized particles, within which the mesostructure develops. This is discussed further below.

Discussion

If a proper understanding is to be achieved of the factors that influence mesostructured silica particle morphology, a realistic model is required of the mechanism of formation of mesostructured precipitates.

Initially, two possible formation pathways for M41S materials were proposed by the Mobil group,[1–3] based on the similarity between the structures of M41S materials and those of lyotropic liquid crystal phases produced in surfactant–water mixtures. In the first "liquid crystal templating model", inorganic material enters the aqueous region of a pre-existing liquid crystal phase and condenses to form inorganic walls. However, most syntheses are carried out at surfactant concentrations well below those at which liquid crystal phases are expected to form and the precipitates arise from

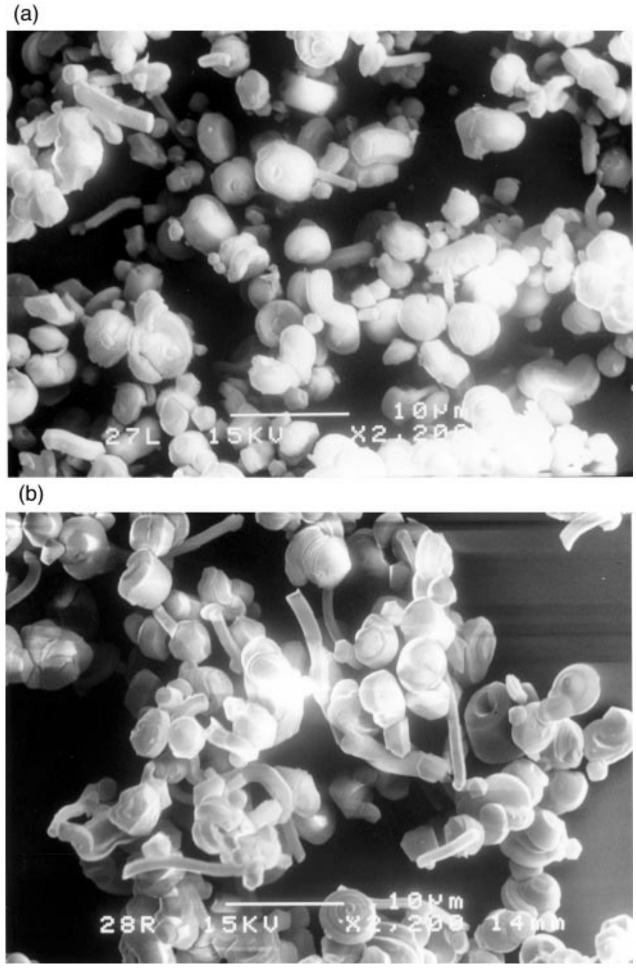

Fig. 10 Scanning electron micrographs of material isolated after (a) 15 min and (b) 24 h from a synthesis mixture of composition 2.2TEOS : 1.1CTAB : 75HCl : 1000H_2O.

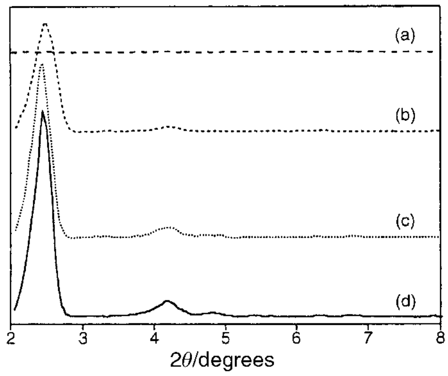

Fig. 11 X-Ray diffraction patterns of material isolated after (a) 15 min, (b) 30 min, (c) 1 h and (d) 24 h from a synthesis mixture of composition 2.2TEOS : 1.1CTAB : 75HCl : 1000H_2O.

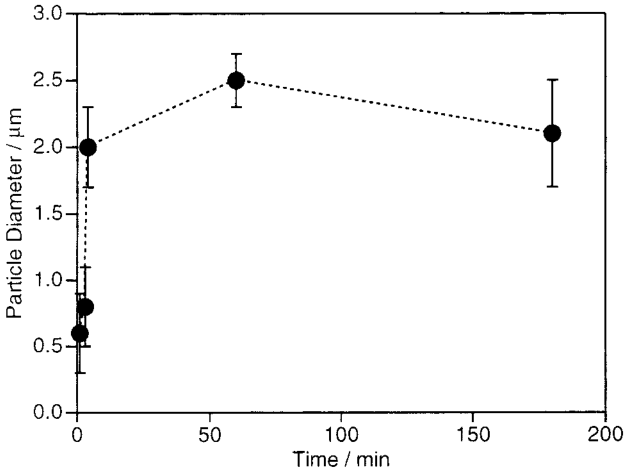

Fig. 12 Dependence of particle size on ageing time for a synthesis mixture of composition 2.0TEOS : 0.25MTES : 1.1CTAB : 75HCl : 1000H_2O.

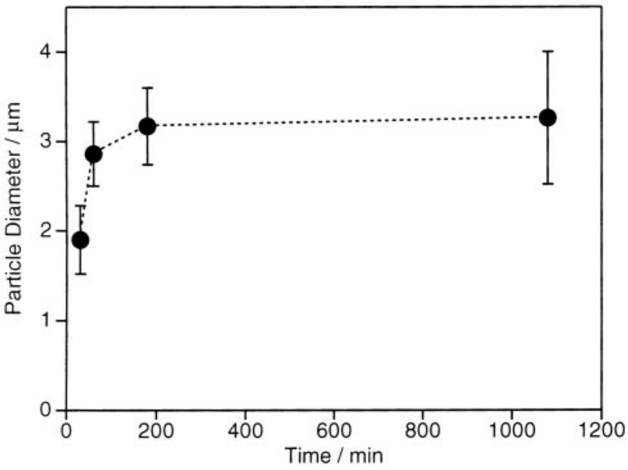

Fig. 13 Dependence of particle size on ageing time for a synthesis mixture of composition 2.2TEOS : 1.1CTAB : 21THF : 75HCl : 1000H_2O.

micellar solutions, so this model cannot generally apply. A number of studies have confirmed that there is no ordered phase present in the original synthesis medium for the preparation of MCM-41.[10,11] An exception is in the approach of Attard, Göltner and co-workers,[12–15] who used bulk liquid crystal phases in the preparation of mesostructured monoliths, but even then the liquid crystal structure was lost during hydrolysis of the silica precursor and reformed subsequently.

In the alternative pathway suggested by the Mobil group,[1–3] which could be called a "micelle assembly model", the inorganic species interact with micelles in solution and mediate an organization process leading to liquid crystal like structures. This idea was developed by Chen *et al.*,[10] who suggested that rodlike inorganic/surfactant complexes are formed which spontaneously pack into an ordered arrangement. Variants of the "micelle assembly model" have been proposed. Regev[16] suggested, on the basis of evidence from cryo-transmission electron micrsocopy, that hydrolysis and condensation may occur on the surface of spherical micelles, decreasing headgroup repulsion and promoting the formation of clusters of elongated micelles. Lee *et al.*[17] proposed that binding of inorganic oligomers promoted a transition from either spherical or rodlike micelles to wormlike micelles, which were then encapsulated by silicate polymers and gradually organised into an ordered array.

Stucky and co-workers[18–20] developed a more general "cooperative assembly model", emphasizing the role of specific interactions between surfactant headgroups and inorganic species. They considered first electrostatic interactions between cationic surfactants and silicate anions, which they referred to as an S^+I^- pathway. They argued that the first stage of the process was multidentate binding of silicate to surfactant, which was followed by cooperative assembly of a liquid crystal like phase, driven by the necessity for charge density matching between silicate and surfactant. The concept was extended to the formation of mesostructures from anionic surfactants and cationic inorganic species (S^-I^+) and, assuming counterion-mediated interactions, from surfactants and inorganic species of the same charge ($S^+X^-I^+$ or $S^-X^+I^-$).[19] Subsequently, Pinnavaia and coworkers[21–23] showed that neutral surfactants could also promote the formation of mesostructured silica, in which case hydrogen bonding was assumed to play a role. Zhao *et al.*[24] suggested a combination of electrostatic and hydrogen bonding interactions could occur in syntheses directed by poly(oxyalkylene) triblock copolymers. Variants of the "cooperative assembly model" have been used by many workers. Holmes *et al.*[25] interpreted an *in situ* FTIR study of the formation of MCM-41 in this way. Galarneau *et al.*[26] used a similar model in interpreting electron paramagnetic resonance results.

Recently, Zana *et al.*[27] used fluorescence probing to test the idea that surfactant counterions may be exchanged for silicate ions, and concluded that only a small fraction of micelle bound counterions are in fact so exchanged. This suggests that the importance of specific interactions between inorganic species and surfactant headgroups may have been overemphasized.

A robust model for the formation of mesostructured precipitates needs to take account of the following points. (1) The present work suggests that the mesostructure may develop within an initially disorganized, or poorly ordered, precipitate. (2) The final product is not a single phase, but a two-phase colloidally structured system; although it is possible that this develops from a homogeneous liquid crystal phase. (3) The process should not be considered as a crystallization; the silica walls are amorphous[28] and order arises only at the colloidal level. (4) Whilst most discussions of the mechanism of formation have focussed on *specific* interactions at the *molecular* level, we are really dealing with a rather *general* phenomenon at the *colloidal* level. A wide range of surfactant types and conditions can give essentially similar products. Furthermore, similar structures to those encountered in inorganic mesostructured precipitates (hexagonal, cubic, lamellar, *etc.*) are observed in many other systems involving amphiphiles, including concentrated surfactant solutions[29,30] and block copolymer blends.[31]

Much has been made of comparisons with binary surfactant/water systems. Less attention has been paid to the fact that the process involves a polymerization leading to an inorganic network polymer, and that it may be instructive to draw lessons from polymer science.

Given a *concentrated* mixture of oligomer, surfactant and water, minimization of Gibbs energy is likely to lead to a colloidally structured system similar to a lyotropic liquid crystal phase. In general, for mixtures involving amphiphiles, microphase separation occurs where there is a thermodynamic driving force for segregation, but separation into two macrophases is prevented by the chemical connectivity within the amphiphile. The precise structure that is obtained depends on the relative amounts of the two phases and on their degree of incompatibility (*e.g.*, for block copolymer melts, weak, intermediate and strong segregation limits have been identified[31]).

The real question is why a concentrated mixture, such as would give rise to microphase separation, should precipitate from dilute solution. It is suggested here that the primary process is one of liquid/liquid, or liquid/liquid crystal, separation.

The phenomenon of liquid/liquid separation in partially miscible liquid mixtures is well known.[32,33] A solution of a non-crystallizable polymer undergoes separation into a dilute and a concentrated phase on cooling in the vicinity of an upper critical solution temperature. If the initial solution is dilute, droplets of the concentrated phase form, giving rise to a cloudy appearance, and in time the droplets normally coalesce to form a separate viscous liquid layer. The cloud point moves to higher temperatures as molar mass increases. If one considers the growth of silica to be a polymerization leading to an insoluble polymer, then one may expect the conditions for phase separation to arise at some point during the polymerization process. The presence of a third component for which there is a favourable interaction with the polymer may further encourage phase separation, and it may also be enriched in the separated phase.

A "phase separation model" for the formation of mesostructured precipitates is thus as follows. (1) Growth of inorganic oligomers gives rise to a thermodynamically unstable mixture (oligomer/surfactant/solvent). (2) Phase separation occurs giving droplets of a second liquid (or liquid crystal) phase rich in oligomer and surfactant. (3) The droplets are colloidally stabilized by electrostatic or steric stabilization; adsorption of excess surfactant may play a role here. (4) Microphase separation occurs within the droplets, giving rise to a mesostructure. (5) Further polymerization fixes the mesostructure.

A full understanding would require knowledge of the equilibrium phase diagram at each instant (it will of course be continually changing as the system changes), coupled with kinetic information for polymerization and phase separation processes. Note that the equilibrium phase diagrams, and consequently the compositions of any separated phases, will be influenced by the relative energies of interaction between oligomer, surfactant and solvent, but it is not essential to postulate strong specific interactions or counterion exchange. When dealing with polymers even quite weak interactions can have a profound effect because they are summed over many segments. This does not mean that the nature of the surfactant and its interactions are unimportant, they will have a profound effect on the outcome of a synthesis, but their influence should be understood in the context of the overall process.

We now consider the issue of particle morphology. A liquid droplet tends to a spherical shape in order to minimize surface energy. Also, an isotropic growth process from a nucleation point gives rise to a spherical structure. A spherical morphology may thus be expected unless other factors have an overriding influence. An internal structure with long range order will force the particle to adopt a regular form, such as the hexagonal morphologies obtained in the present work. However, a wide variety of overall shapes (extended, curled, *etc.*) may represent small fluctuations from an energy minimum, so a mixture may arise, as was observed here. Whether a spherical morphology or a more regular form is obtained is expected to depend on the balance between the rate of polymerization of inorganic species and the rate of mesostructure formation. If the polymerization is slow relative to mesostructure formation, there is time for a highly ordered mesostructure to develop. However, if the polymerization is relatively fast, the viscosity will increase and mobility be restricted before the mesostructure can be perfected. Other factors may also influence morphology, such as colloid stability, as aggregation may give rise to irregular particles.

Acknowledgements

We are grateful to EPSRC and Smart Chemical Company for provision of a CASE studentship for H. B. S. C. and to Dr F. Heatley for assistance with NMR.

References

1 C. T. Kresge, M. E. Leonowicz, W. J. Roth, J. C. Vartuli and J. S. Beck, *Nature*, 1992, **359**, 710.
2 J. S. Beck, J. C. Vartuli, W. J. Roth, M. E. Leonowicz, C. T. Kresge, K. D. Schmitt, C. T-W. Chu, D. H. Olson, E. W. Sheppard, S. B. McCullen, J. B. Higgins and J. L. Schlenker, *J. Am. Chem. Soc.*, 1992, **114**, 10834.
3 S. B. McCullen, J. C. Vartuli, C. T. Kresge, W. J. Roth, J. S. Beck, K. D. Schmitt, M. E. Leonowicz, J. L. Schlenker, S. S. Shih and J. D. Lutner, in *Access in Nanoporous Materials*, ed. T. J. Pinnavaia and M. F. Thorpe, Plenum Press, New York, 1995, pp. 1–11.
4 Y. A. I. Abu-Lebdeh, P. M. Budd and V. M. Nace, *J. Mater. Chem.*, 1998, **8**, 1839.
5 Q. Huo, J. Feng, F. Schüth and G. D. Stucky, *Chem. Mater.*, 1997, **9**, 14.
6 H. Yang, G. Vovk, N. Coombs, I. Sokolov and G. A. Ozin, *J. Mater. Chem.*, 1998, **8**, 743.
7 H. Yang, N. Coombs and G. A. Ozin, *Nature*, 1997, **386**, 692.
8 S. Schacht, Q. Huo, I. G. Voigt-Martin, G. D. Stucky and F. Schüth, *Science*, 1996, **273**, 768.
9 S. Dirè, E. Pagani, F. Babonneau, R. Ceccato and G. Carturan, *J. Mater. Chem.*, 1997, **7**, 67.
10 C-Y. Chen, S. L. Burkett, H-X. Li and M. E. Davis, *Microporous Mater.*, 1993, **2**, 27.
11 S. O'Brien, R. J. Francis, A. Fogg, D. O'Hare, N. Okazake and K. Kuroda, *Chem. Mater.*, 1999, **11**, 1822.
12 G. S. Attard, J. C. Glyde and C. G. Göltner, *Nature*, 1995, **378**, 366.
13 C. G. Göltner and M. Antionetti, *Adv. Mater.*, 1997, **9**, 431.
14 C. G. Göltner, B. Berton, E. Krämer and M. Antionetti, *Chem. Commun.*, 1998, 2287.
15 C. G. Göltner, S. Henke, M. C. Weissenberger and M. Antonetti, *Angew. Chem., Int. Ed.*, 1998, **37**, 613.
16 O. Regev, *Langmuir*, 1996, **12**, 4940.
17 Y. S. Lee, D. Surjadi and J. F. Rathman, *Langmuir*, 1996, **12**, 6202.
18 A. Monnier, F. Schüth, Q. Huo, D. Kumar, D. Margolese, R. S. Maxwell, G. D. Stucky, M. Krishnamurty, P. Petroff, A. Firouzi, M. Janicke and B. F. Chmelka, *Science*, 1993, **261**, 1299.
19 Q. Huo, D. J. Margolese, U. Ciesla, D. G. Demuth, P. Feng, T. E. Gier, P. Sieger, A. Firouzi, B. F. Chmelka, F. Schüth and G. D. Stucky, *Chem. Mater.*, 1994, **6**, 1176.
20 A. Firouzi, D. Kumar, L. M. Bull, T. Besier, P. Sieger, Q. Huo, S. A. Walker, J. A. Zasadzinski, C. Glinka, J. Nicol, D. Margolese, G. D. Stucky and B. F. Chmelka, *Science*, 1995, **267**, 1138.
21 P. T. Tanev and T. J. Pinnavaia, *Science*, 1995, **267**, 865.
22 P. T. Tanev and T. J. Pinnavaia, *Chem. Mater.*, 1996, **8**, 2068.
23 S. A. Bagshaw, E. Prouzet and T. J. Pinnavaia, *Science*, 1995, **269**, 1242.
24 D. Zhao, J. Feng, Q. Huo, N. Melosh, G. H. Fredrickson, B. F. Chmelka and G. D. Stucky, *Science*, 1998, **279**, 548.
25 S. M. Holmes, V. L. Zholobenko, A. Thursfield, R. J. Plaisted, C. S. Cundy and J. Dwyer, *J. Chem. Soc., Faraday Trans.*, 1998, **94**, 2025.
26 A. Galarneau, F. Di Renzo, F. Fajula, L. Mollo, B. Fubini and M. F. Ottaviani, *J. Colloid Interface Sci.*, 1998, **201**, 105.
27 R. Zana, J. Frasch, M. Soulard, B. Lebeau and J. Patarin, *Langmuir*, 1999, **15**, 2603.
28 C-Y. Chen, H-X. Li and M. E. Davis, *Microporous Mater.*, 1993, **2**, 17.
29 J. H. Clint, *Surfactant Aggregation*, Blackie, Glasgow, 1992.
30 R. G. Laughlin, *The Aqueous Phase Behaviour of Surfactants*, Academic, London, 1994.
31 I. W. Hamley, *The Physics of Block Copolymers*, Oxford University Press, Oxford, 1998.
32 J. H. Hildebrand and R. L. Scott, *Regular Solutions*, Prentice-Hall, Englewood Cliffs, 1962.
33 H. Tompa, *Polymer Solutions*, Butterworths, London, 1956.